


Monitoring Enzyme Activity Using a Diamagnetic Chemical Exchange Saturation Transfer Magnetic Resonance Imaging Contrast Agent

Guanshu Liu,^{†,‡} Yajie Liang,^{‡,§} Amnon Bar-Shir,^{‡,§} Kannie W. Y. Chan,^{‡,§} Chulani S. Galpoththawela,^{‡,§} Segun M. Bernard,^{‡,§} Terence Tse,[‡] Nirbhay N. Yadav,^{†,‡} Piotr Walczak,^{‡,§} Michael T. McMahon,^{†,‡} Jeff W. M. Bulte,^{‡,§} Peter C. M. van Zijl,^{†,‡} and Assaf A. Gilad^{†,‡,§,†}

[†]F. M. Kirby Research Center for Functional Brain Imaging, Kennedy Krieger Research Institute, Baltimore, Maryland 21205, United States

[‡]Russell H. Morgan Department of Radiology and [§]Cellular Imaging Section and Vascular Biology Program, Institute for Cell Engineering, The Johns Hopkins University School of Medicine, Baltimore, Maryland 21205, United States

 Supporting Information

ABSTRACT: Chemical exchange saturation transfer (CEST) is a new approach for generating magnetic resonance imaging (MRI) contrast that allows monitoring of protein properties in vivo. In this method, a radiofrequency pulse is used to saturate the magnetization of specific protons on a target molecule, which is then transferred to water protons via chemical exchange and detected using MRI. One advantage of CEST imaging is that the magnetizations of different protons can be specifically saturated at different resonance frequencies. This enables the detection of multiple targets simultaneously in living tissue. We present here a CEST MRI approach for detecting the activity of cytosine deaminase (CDase), an enzyme that catalyzes the deamination of cytosine to uracil. Our findings suggest that metabolism of two substrates of the enzyme, cytosine and 5-fluorocytosine (5FC), can be detected using saturation pulses targeted specifically to protons at +2 ppm and +2.4 ppm (with respect to water), respectively. Indeed, after deamination by recombinant CDase, the CEST contrast disappears. In addition, expression of the enzyme in three different cell lines exhibiting different expression levels of CDase shows good agreement with the CDase activity measured with CEST MRI. Consequently, CDase activity was imaged with high-resolution CEST MRI. These data demonstrate the ability to detect enzyme activity based on proton exchange. Consequently, CEST MRI has the potential to follow the kinetics of multiple enzymes in real time in living tissue.

To study proteins and enzymes in their natural context in living organisms, a noninvasive imaging technique with high spatial and temporal resolution is required. Such resolution can be achieved using magnetic resonance imaging (MRI), which has been used extensively in the last two decades for anatomical, functional, and dynamic imaging. Detection with MRI relies on contrast in the MRI signal between the tissue of interest and its surrounding tissue, which can be further enhanced by expression of certain exogenous proteins that increase MRI contrast. Recently, a new type of MRI contrast that relies on direct chemical exchange of protons with bulk water has been developed. A variety of organic molecules^{1–6} and lanthanide complexes^{7–10} possessing protons that exchange rapidly with the surrounding water

protons have been suggested as powerful new contrast agents. These exchangeable protons can be “magnetically tagged” using a radiofrequency saturation pulse applied at their resonance frequency. The tagged protons exchange with the protons of surrounding water molecules and consequently reduce the MRI signal. This itself would not be visible at the low concentrations of solute, but the exchanged protons are replaced with fresh, unsaturated protons and the same saturation process is repeated. After several seconds of this process, the effect becomes amplified, and very low concentrations of agents can be detected. Hence, these agents are termed chemical exchange saturation transfer (CEST) contrast agents. One main advantage of CEST MRI is the possibility of generating MRI contrast using bio-organic molecules such as polysaccharides (sugars), proteins, enzymes, and substrates that can be noninvasively detected in tissue.^{3,4,11,12}

CEST MRI was previously used to detect enzyme activity using paramagnetic (PARACEST) substrates, which rely on a shift in the water exchange frequency after the enzymatic reaction.^{10,13–15} Here we used the enzyme cytosine deaminase (CDase) to demonstrate the feasibility of using CEST MRI as a specific tool for noninvasive real-time imaging of enzyme activity using metal-free bio-organic diamagnetic substrates (DIACEST). CDase is expressed exclusively in bacteria and fungi as an important part of the pyrimidine salvage pathway. CDase catalyzes the conversion of cytosine to uracil through the removal of an amine group, or “deamination”. It can also convert the prodrug 5-fluorocytosine (5FC) into the chemotherapeutic agent 5-fluorouracil (5FU), making it a promising enzyme/prodrug system for cancer therapy.¹⁶ Because CDase activity is absent in mammalian cells, the administration of 5FC is not likely to result in significant toxicity to normal tissue. Since amine groups contain two exchangeable protons, we hypothesized that deamination of cytosine or 5FC by CDase to generate uracil or 5FU should be detectable by CEST MRI (Figure 1).

We first determined whether CEST MRI could detect the CDase substrates and products with sufficient sensitivity under physiological conditions. We examined the CEST contrast generated by cytosine, uracil, 5FC, and 5FU over a range of concentrations at pH 7.4 and 37 °C. The solid lines in Figure 2a,b represent the CEST spectra, in which the water proton signal is plotted as a function of

Received: May 23, 2011

Published: September 16, 2011

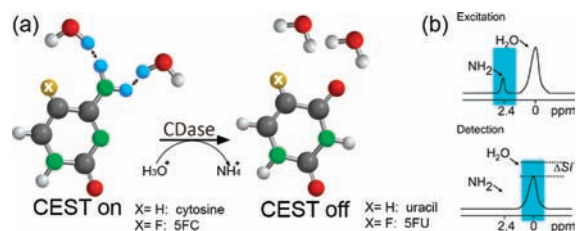


Figure 1. (a) CDase catalyzes the deamination of cytosine and 5FC to uracil and 5FU, respectively. (b) A frequency-selective saturation pulse is applied to label the amine protons (cyan) of cytosine or 5FC. The labeled protons exchange with water protons, leading to a reduction in MRI signal intensity in a frequency-selective manner, generating CEST contrast.

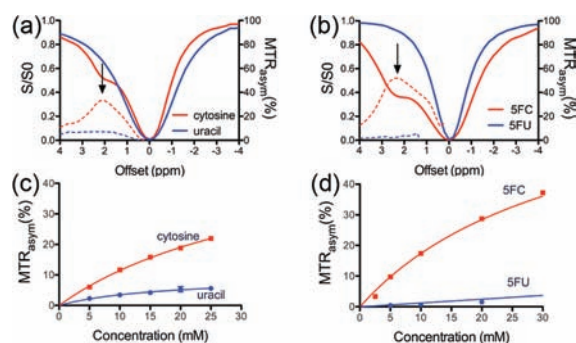


Figure 2. CEST properties of cytosine, uracil, 5FC, and 5FU at 9.4 T, pH 7.4, and 37 °C. (a, b) CEST spectra (solid lines) and MTR_{asym} plots (dashed lines) of 40 mM (a) cytosine (red) and uracil (blue) and (b) 5FC (red) and 5FU (blue). Arrows point to the maximal MTR_{asym} . (c, d) Concentration dependences of MTR_{asym} at 2 ppm and 2.4 ppm are shown for (c) cytosine and uracil and (d) 5FC and 5FU, respectively.

saturation frequency. The dashed lines represent plots of MTR_{asym} , a measure of CEST contrast defined by $MTR_{asym} = (S^{-\Delta\omega} - S^{\Delta\omega})/S_0$, in which $S^{-\Delta\omega}$ and $S^{\Delta\omega}$ are the MRI signal intensities after saturation at $-\Delta\omega$ and $+\Delta\omega$, where $\Delta\omega$ is the frequency offset from the water proton frequency (set at 0 ppm by convention), and S_0 is the intensity in the absence of a saturation pulse. The maximal MTR_{asym} values for cytosine and 5FC were obtained at offsets of +2 ppm and +2.4 ppm, respectively. In contrast, uracil and 5FU, which do not have an NH_2 group, showed only limited and non-frequency-specific MTR_{asym} that is probably due to the rapidly exchanging 1- or 3-imino NH protons, although this has not been confirmed. Figure 2c,d shows the dynamic range of these substrate concentrations that can be detected with CEST MRI. These findings indicate that CEST MRI is suitable for monitoring the deamination of cytosine and 5FC.

We determined the exchange rate (k_{ex}) of the amine protons of cytosine to be 8.1×10^2 Hz by measuring MTR_{asym} as a function of saturation time² (Figure S1a in the Supporting Information). This was in good agreement with the value of 9.3×10^2 Hz determined using an alternative approach, the frequency-labeled exchange (FLEX) transfer method¹⁷ (Figure S2). For the amine proton of 5FC, k_{ex} was found to be 1.8×10^3 Hz (Figure S1b). For both cytosine and 5FC, k_{ex} is on the order of magnitude of the frequency difference with water ($\Delta\omega$), in the intermediate exchange range. Notably, CEST can still detect such rapidly exchanging protons, such as OH groups,⁴ as long as some partial saturation can be achieved while the proton is at the correct frequency. This is an advantage over conventional MRI, where it would not be detectable.

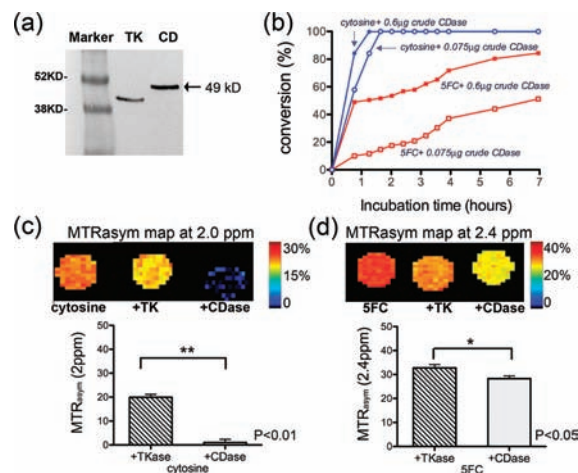


Figure 3. Monitoring of recombinant CDase activity using CEST MRI. (a) Western blot using an anti-six-histidine-tag antibody of protein extracts from *E. coli* engineered to express CD or HSV1-tk (TK). (b) Deamination of cytosine and 5FC (20 mM) by crude CDase extracts measured using CEST MRI at 37 °C and 9.4T. Conversion was quantified as $(1 - MTR_{asym}^t/MTR_{asym}^0) \times 100\%$, where MTR_{asym}^t and MTR_{asym}^0 are the contrasts at time t and at $t = 0$, respectively. (c, d) Maps and statistical analysis (two-tailed unpaired Student's t test; $n = 3$) of 20 mM (c) cytosine and (d) 5FC incubated with CDase (0.6 μ g crude protein) for 24 h.

Next, we evaluated the detection of recombinant CDase activity with CEST MRI. The gene encoding the *Escherichia coli* CDase (*CodA*) was cloned into an expression vector (pEXP5-CT; Invitrogen) in a reading frame with a six-histidine C-terminal tag under the regulation of the T7 promoter. The gene encoding the herpes simplex virus type-1 thymidine kinase (HSV1-tk) was used as a control. Both enzymes were over-expressed in *E. coli* (BL21), and a crude protein extract was used to measure enzymatic activity with MRI. As shown in Figure 3b, with recombinant CDase, substrate conversions could be measured for both cytosine and 5FC. Figure 3c,d demonstrates that the reduction in MTR_{asym} in the presence of CDase is significantly larger than that in the presence of the control enzyme HSV1-tk. While the conversion of cytosine was nearly complete after 24 h, this was not the case for 5FC. This can be attributed to the lower specificity of CDase toward 5FC relative to its natural substrate cytosine.¹⁸ A slight reduction in MTR_{asym} was also observed in the extract containing recombinant HSV1-tk, possibly resulting from endogenous CDase activity.

Therefore, we tested the CDase activity in mammalian cells that do not express endogenous CDase. A lentivirus that encodes CDase under the CMV promoter was constructed. The lentivirus was used to transduce three different cell lines in culture. As shown in Figure 4a, the cell lines expressed different levels of CDase. Human embryonic kidney (HEK293FT) cells expressed the highest amount, 9L rat glioma expressed an intermediate level, and C17.2 mouse neural stem cells failed to express the enzyme at a detectable level.

For each cell type, the same number of transduced or untransduced [wild-type (WT)] cells were plated (5.6×10^6 HEK293FT, 10^6 9L, and 1.4×10^6 C17.2 cells). Fresh culture medium containing 7 mM cytosine or 10 mM 5FC was added to the cells, and 50 μ L of the culture medium was collected at different time points up to 48 h and measured with CEST MRI in capillaries, as described previously.¹⁹ Figure 4b demonstrates a significant

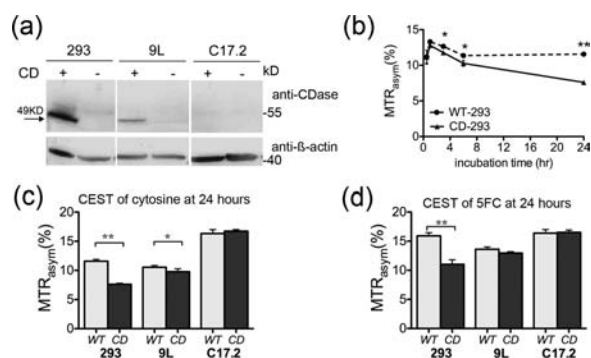


Figure 4. Detection of CDase in mammalian cells. (a) Western blot of wild-type (WT) or CDase-transduced HEK293FT (293), 9L, and C17.2 cells stained with anti-CDase and anti- β -actin for total protein. (b) MTR_{asym} of the supernatant of culture media of HEK293FT cells transduced with CD (CD-293) or control (WT-293) collected at different time points after incubation with 7 mM cytosine. (c, d) MTR_{asym} of the culture media 24 h after incubation with (c) 7 mM cytosine and (d) 10 mM 5FC at 2.0 and 2.4 ppm, respectively. In (c) and (d), WT and CD represent transduced and nontransduced cells respectively. * indicates $p < 0.05$ and ** indicates $p < 0.01$ (two-tailed unpaired Student's t test).

difference in MTR_{asym} for transduced and nontransduced HEK293FT cells as early as 4 h after incubation with 7 mM cytosine. This is in good agreement with the high expression level of CDase by those cells. In contrast, for cells treated with 10 mM 5FC, a significant difference in MTR_{asym} was observed only after 24 h (Figure S3). Figure 4b shows an initial increase in MTR_{asym} at the initial time points. We tentatively attribute this to small changes in the ratio of enzyme to substrate, which may be the result of a reduction in the volume of the solution due to the sampling methods or of evaporation of minute amounts of the medium over time. Alternatively, changes in the pH of the cell culture medium may affect MTR_{asym} . Nevertheless, the experimental results show a significant difference between CDase-expressing cells and the controls, indicating the ability to monitor enzyme activity directly. Figure 4c,d shows the difference in MTR_{asym} for all cell lines after 24 h of incubation with cytosine and 5FC, respectively. At this time point, the HEK293FT cells showed a significant difference in MTR_{asym} for both cytosine and 5FC. The 9L cells, which exhibited an intermediate expression level of CDase, showed a moderate reduction of MTR_{asym} only for cytosine but not for 5FC. The C17.2 cells, which had undetectable CDase expression, showed no difference in MTR_{asym} at this time point. (A complete time course of CEST MRI, validation with ^{19}F -MR spectroscopy, and a cell viability assay can be found in Figures S3–S5.)

Immunoprotected cells have been evaluated as a new therapeutic alternative, for example, for pancreatic islet cell replacement in diabetic patients. In this approach, cells are encapsulated with alginate that enables passage of essential factors (e.g., nutrients and insulin) but protects cells from attack by the body's immune system. Several methods for monitoring encapsulated cells after transplantation have been successfully developed.^{20–23} Nevertheless, a noninvasive method for visualizing the viability of the transplant would be highly beneficial. In order to evaluate the feasibility of this method in cells, we encapsulated HEK293FT expressing CDase or nonexpressing control cells. As shown in Figure 5, upon incubation with 5FC, only the CDase-expressing cells (CD-293) showed conversion of 5FC (initial concentration of 30 mM) within the first 3 h. On the basis

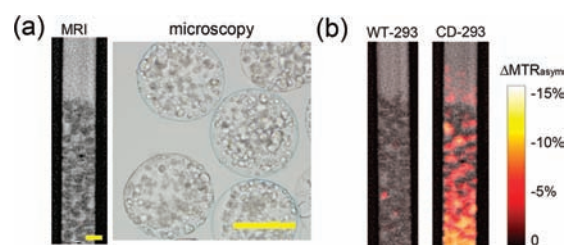


Figure 5. Imaging of cellular enzyme activity: CEST MRI of HEK293FT cells transduced with CDase (CD-293) or control cells (WT-293) encapsulated within alginate (200–300 cells per microcapsule). (a) High-resolution MR image ($90 \times 50 \mu\text{m}$, left) with corresponding microscopy image (right). Scale bars = $400 \mu\text{m}$. (b) Conversion map overlaid on T2-weighted images, clearly showing that CD-293 cells but not WT-293 cells effectively converted 5FC to 5FU with a concurrent change in CEST signal.

of the cytotoxic mechanism of 5FU, it is unlikely that there is a contribution of cell death to the change in MTR_{asym} . These findings indicate that CDase activity can be imaged at the macrocellular level in 3D culture. In addition, the CDase may be used not only to monitor the transplant viability but also as a suicide gene that can be used to eradicate transplanted cells in case of tumorigenic transformation of the transplanted cells.²⁴

This study demonstrates that the activity of the enzyme CDase can be monitored using CEST MRI. Previously, such detection was possible using ^{19}F NMR spectroscopy²⁵ and ^{19}F NMR spectroscopic imaging,²⁶ which rely on a change in chemical shift upon conversion of 5FC to 5FU. One advantage of using CEST MRI is that there is no need to use a toxic prodrug (5FC). Instead, the CDase's natural substrate, cytosine, can be used for imaging. This allows repetitive measurements and the use of CDase as a reporter gene. Another advantage is that CEST MRI can be used to monitor multiple enzymes simultaneously as long as their substrates have exchangeable protons that resonate at distinct frequencies. This property is relevant for studying gene networks, for example, in signal transduction cascade pathways.

An additional potential application may be real-time monitoring of the efficiency of therapeutic gene delivery and expression. As CDase has already entered the clinic for cancer gene therapy,²⁷ such real-time monitoring may aid in predicting treatment outcomes. Since different cells or tumors may express differential levels of CDase, different patients may respond differently. Hence, real-time monitoring of enzymatic activity by CEST MRI could guide personalized medicine. Nevertheless, before this method can be fully translated, several hurdles must be overcome. Among these is optimization of the sensitivity of the substrates. The sensitivity in vivo depends on the expression levels of the enzyme, the cell density, and accessibility of the substrate to the CDase-expressing cells. Our in vitro data indicate that recombinant CDase from 10^6 mammalian cells is sufficient to reduce MTR_{asym} significantly upon incubation with 7 mM cytosine or 10 mM 5FC. This number of cells is on the same order of magnitude as that used in cell-mediated CDase cancer gene therapy in vivo studies.²⁸ The signal-to-noise ratio (SNR) of CEST MRI is ~ 80 , which is less than the SNR of 160 for ^{19}F NMR (Figures S3 and S4 and Table S1). However, for the same level of CDase expressed by 9L cells, a relative change in MTR_{asym} of 12% was observed after 48 h incubation with 5FC, compared with an 8.5% change measured using ^{19}F NMR. With cytosine as the

substrate under the same conditions, a much higher change (i.e., 50%) was observed with CEST MRI. Thus, the sensitivity of CEST MRI is comparable to that of conventional ^{19}F NMR.²⁵

A change of >5% in MTR_{asym} was detected from 200–300 cells encapsulated in each 400–500 μm diameter alginate bead. As a 3D multicellular spheroid with a diameter of 300 μm consists of 3900 cells,²⁹ CEST MRI is expected to allow measurement of CDase activity even when only 5–10% of the cells express the enzyme. Taken together, these results show that the present CEST MRI approach is expected to be sufficiently sensitive for future preclinical or clinical applications.

In addition, CEST contrast is highly dependent on the exchange rate,³⁰ which can be modified using chemical modifications. This would be aimed toward increasing MTR_{asym} of the amine protons as well as the imino protons. The latter can be achieved by reducing the exchange rate at physiological pH, which may produce CEST contrast at 5–6 ppm. This would allow reduction of the applied B1, thereby decreasing the background from endogenous magnetization transfer effects as well as from direct water saturation. Shortening the image acquisition time is also required for improving the temporal resolution, which would allow more accurate dynamic measurement of the enzyme activity. Moreover, the enzyme turnover rate for substrates can be improved using genetic manipulations. The turnover rate was significantly improved when the entire gene³¹ or just its active site³² was subjected to directed evolution. It is noteworthy that T2 exchange effects may cause CEST agents to behave as T2 agents, resulting in darkening of the image.³³ However, this is not a problem for the current agents at the low concentrations used and the chemical shift difference for these DIACEST agents. Finally, the detection may be improved by controlling the levels of the agents, for example by sustained release.³⁴

In summary, we have demonstrated that CEST MRI, a novel approach for producing contrast based on proton exchange, can be used for direct real-time monitoring of CDase activity.

ASSOCIATED CONTENT

S Supporting Information. Experimental procedures, MRI acquisition, and data processing methods. This material is available free of charge via the Internet at <http://pubs.acs.org>.

AUTHOR INFORMATION

Corresponding Author

assaf.gilad@jhu.edu

ACKNOWLEDGMENT

This work was supported by NIH Grants EB008769, NS065284, EB005252, EB012590, EB006394, and EB015032. The authors thank Dr. Raag D. Airan for his comments on the manuscript.

REFERENCES

- (1) Ward, K. M.; Aletras, A. H.; Balaban, R. S. *J. Magn. Reson.* **2000**, *143*, 79.
- (2) McMahon, M. T.; Gilad, A. A.; Zhou, J.; Sun, P. Z.; Bulte, J. W.; van Zijl, P. C. *Magn. Reson. Med.* **2006**, *55*, 836.
- (3) Ling, W.; Regatte, R. R.; Navon, G.; Jerschow, A. *Proc. Natl. Acad. Sci. U.S.A.* **2008**, *105*, 2266.
- (4) van Zijl, P. C.; Jones, C. K.; Ren, J.; Malloy, C. R.; Sherry, A. D. *Proc. Natl. Acad. Sci. U.S.A.* **2007**, *104*, 4359.
- (5) van Zijl, P. C.; Yadav, N. N. *Magn. Reson. Med.* **2011**, *65*, 927.

- (6) Zhou, J.; Payen, J. F.; Wilson, D. A.; Traystman, R. J.; van Zijl, P. C. *M. Nat. Med.* **2003**, *9*, 1085.
- (7) Sherry, A. D.; Woods, M. *Annu. Rev. Biomed. Eng.* **2008**, *10*, 391.
- (8) Terreno, E.; Castelli, D. D.; Cravotto, G.; Milone, L.; Aime, S. *Invest. Radiol.* **2004**, *39*, 235.
- (9) Vinogradov, E.; He, H.; Lubag, A.; Balschi, J. A.; Sherry, A. D.; Lenkinski, R. E. *Magn. Reson. Med.* **2007**, *58*, 650.
- (10) Yoo, B.; Pagel, M. D. *J. Am. Chem. Soc.* **2006**, *128*, 14032.
- (11) Gilad, A. A.; McMahon, M. T.; Walczak, P.; Winnard, P. T., Jr.; Raman, V.; van Laarhoven, H. W.; Skoglund, C. M.; Bulte, J. W.; van Zijl, P. C. *Nat. Biotechnol.* **2007**, *25*, 217.
- (12) Haris, M.; Cai, K.; Singh, A.; Hariharan, H.; Reddy, R. *Neuroimage* **2011**, *54*, 2079.
- (13) Suchy, M.; Ta, R.; Li, A. X.; Wojciechowski, F.; Pasternak, S. H.; Bartha, R.; Hudson, R. H. E. *Org. Biomol. Chem.* **2010**, *8*, 2560.
- (14) Chauvin, T.; Durand, P.; Bernier, M.; Meudal, H.; Doan, B.-T.; Noury, F.; Badet, B.; Beloeil, J.-C.; Tóth, É. *Angew. Chem., Int. Ed.* **2008**, *47*, 4370.
- (15) Yoo, B.; Raam, M. S.; Rosenblum, R. M.; Pagel, M. D. *Contrast Media Mol. Imaging* **2007**, *2*, 189.
- (16) Aghi, M.; Hochberg, F.; Breakefield, X. *J. Gene Med.* **2000**, *2*, 148.
- (17) Friedman, J. I.; McMahon, M. T.; Stivers, J. T.; Van Zijl, P. C. *J. Am. Chem. Soc.* **2010**, *132*, 1813.
- (18) Porter, D. J. *Biochim. Biophys. Acta* **2000**, *1476*, 239.
- (19) Liu, G.; Gilad, A. A.; Bulte, J. W.; van Zijl, P. C.; McMahon, M. T. *Contrast Media Mol. Imaging* **2010**, *5*, 162.
- (20) Arifin, D. R.; Long, C. M.; Gilad, A. A.; Alric, C.; Roux, S. p.; Tillemont, O.; Link, T. W.; Arepally, A.; Bulte, J. W. M. *Radiology* **2011**, *260*, 790.
- (21) Barnett, B. P.; Arepally, A.; Karmarkar, P. V.; Qian, D.; Gilson, W. D.; Walczak, P.; Howland, V.; Lawler, L.; Lauzon, C.; Stuber, M.; Kraitchman, D. L.; Bulte, J. W. *Nat. Med.* **2007**, *13*, 986.
- (22) Barnett, B. P.; Arepally, A.; Stuber, M.; Arifin, D. R.; Kraitchman, D. L.; Bulte, J. W. *Nat. Protoc.* **2011**, *6*, 1142.
- (23) Kim, J.; Arifin, D. R.; Muja, N.; Kim, T.; Gilad, A. A.; Kim, H.; Arepally, A.; Hyeon, T.; Bulte, J. W. *Angew. Chem., Int. Ed.* **2011**, *50*, 2317.
- (24) Cao, F.; Drukker, M.; Lin, S.; Sheikh, A. Y.; Xie, X.; Li, Z.; Connolly, A. J.; Weissman, I. L.; Wu, J. C. *Cloning Stem Cells* **2007**, *9*, 107.
- (25) Aboagye, E.; Artemov, D.; Senter, P.; Bhujwala, Z. *Cancer Res.* **1998**, *58*, 4075.
- (26) Gade, T. P.; Koutcher, J. A.; Spees, W. M.; Beattie, B. J.; Ponomarev, V.; Doubrovina, M.; Buchanan, I. M.; Beresten, T.; Zakian, K. L.; Le, H. C.; Tong, W. P.; Mayer-Kuckuk, P.; Blasberg, R. G.; Gelovani, J. G. *Cancer Res.* **2008**, *68*, 2878.
- (27) Freytag, S. O.; Khil, M.; Stricker, H.; Peabody, J.; Menon, M.; DePeralta-Venturina, M.; Nafziger, D.; Pegg, J.; Paielli, D.; Brown, S.; Barton, K.; Lu, M.; Aguilar-Cordova, E.; Kim, J. H. *Cancer Res.* **2002**, *62*, 4968.
- (28) Shimato, S.; Natsume, A.; Takeuchi, H.; Wakabayashi, T.; Fujii, M.; Ito, M.; Ito, S.; Park, I.; Bang, J.; Kim, S. *Gene Ther.* **2007**, *14*, 1132.
- (29) Sutherland, R. M. *Science* **1988**, *240*, 177.
- (30) Snoussi, K.; Bulte, J. W.; Gueron, M.; van Zijl, P. C. *Magn. Reson. Med.* **2003**, *49*, 998.
- (31) Mahan, S. D.; Ireton, G. C.; Knoeber, C.; Stoddard, B. L.; Black, M. E. *Protein Eng., Des. Sel.* **2004**, *17*, 625.
- (32) Fuchita, M.; Ardiani, A.; Zhao, L.; Serve, K.; Stoddard, B. L.; Black, M. E. *Cancer Res.* **2009**, *69*, 4791.
- (33) Soesbe, T. C.; Merritt, M. E.; Green, K. N.; Rojas-Quijano, F. A.; Sherry, A. D. *Magn. Reson. Med.* [Online early access]. DOI: 10.1002/mrm.22938. Published Online: May 23, 2011.
- (34) Choi, J.; Kim, K.; Kim, T.; Liu, G.; Bar-Shir, A.; Hyeon, T.; McMahon, M. T.; Bulte, J. W. M.; Fisher, J. P.; Gilad, A. A. *J. Controlled Release* [Online early access]. DOI: 10.1016/j.jconrel.2011.06.035. Published Online: July 8, 2011.